

## DESIGN OF A MOLYBDENUM BASED OXYGEN SENSOR TO ASSIST IN THE CHARACTERIZATION OF CANDU<sup>®</sup> NUCLEAR FUELS AS A FUNCTION OF BURNUP

R.A. Barry\*, J. Scott and E.C. Corcoran

Royal Military College of Canada, Kingston, Ontario, Canada  
11 General Crerar Crescent, Kingston, ON, K7K 7B4, \*[Aaron.Barry@rmc.ca](mailto:Aaron.Barry@rmc.ca)

**ABSTRACT** - In a CANDU<sup>®</sup> reactor, ceramic uranium dioxide ( $UO_2$ ) fuel pellets are contained in Zircaloy-4 cladding. On the rare occurrence of a fuel defect, heavy water ( $D_2O$ ) steam can come into direct contact with the fuel resulting in oxidation of the fuel, fission products, and activation products [1]. The objective of this project is to understand the fundamental relationship between the partial pressure of oxygen ( $pO_2$ ), non-stoichiometric  $UO_2$ , and specific mixtures of fission product oxides. A special emphasis will be placed on the molybdenum ( $Mo$ ) fission products because of the existing relationship between  $Mo$  oxidation states and  $pO_2$ . An increased understanding of the  $U-Mo-O$  relationship could lead to a method of estimating the local  $pO_2$  exposure based on the quantities of the different forms in which  $Mo$  is found ( $Mo$ ,  $MoO_{2+x}$ ,  $UMoO_6$ , etc.). In future, this method could be employed as a forensic tool to evaluate the propagation of oxygen through a defective fuel element with increased spatial resolution or to confirm burnup in non-defective fuel.

### 1. Introduction

The properties and behaviours of a nuclear fuel are largely dependent on fuel chemistry. An in-core fuel is a complex system of non-stoichiometric uranium dioxide ( $UO_{2+x}$ ) fuel and activation and fission products. The fuel chemistry is modelled by computer codes, which combine the thermodynamic properties of individual systems, mass balance, and chemical and environmental conditions of the fuel to model the complex system.

The RMCC thermodynamic fuel model [2] determines fuel conditions at equilibrium, specifically the oxidation of the fuel in the presence of fission and activation products. It sets the framework for complete kinetic models. Its basis is the well-understood relationship between  $pO_2$  and  $UO_{2+x}$ . However, the relationship between  $pO_2$  and the fission / activation products in a uranium system still requires further characterization.

This project focuses on establishing an improved relationship between  $pO_2$  and the oxide to metal ratio of the  $Mo-O$  and  $U-Mo-O$  systems. The benefits of this relationship are three-fold:

- i. The collection of data used to establish these relationships can be used to benchmark and validate components of the RMCC thermodynamic fuel model;
- ii. These relationships could assist in the development of a stand-alone forensic tool that could track the propagation of oxygen through a defective fuel element by estimating the local  $pO_2$  exposure based on the speciation of  $Mo$  ( $Mo$ ,  $MoO_{2+x}$ ,  $UMoO_6$ , etc.); and
- iii. These relationships can potentially be used to confirm non-defective fuel burnup as the oxide to metal ratio is a function of  $pO_2$  and  $Mo$  concentration, which are both related to burnup.

## 2. Background

### 2.1 Fission and Modelling

CANDU<sup>®</sup> reactor fuel is natural  $UO_2$  sintered into ceramic fuel pellets. The fuel pellets are loaded into Zircaloy-4 tubes, backfilled with helium gas and sealed to form fuel elements, which are assembled into bundles [3]. The fresh  $UO_2$  fuel undergoes fission and a variety of fission and activation products begin to accumulate. The result is a complex fuel system with components that span the majority of the periodic table[2].

On the rare occurrence of a fuel defect<sup>\*</sup>,  $D_2O$  coolant can breach the Zircaloy-4 cladding, flash to steam and dissociate into oxygen ( $O_2$ ) and hydrogen ( $H_2$ ) gas [4]. Oxidation of the fuel and fission and activation products can then occur. The amount of oxidation is directly related to the amount of  $O_2$  (i.e., the  $pO_2$ ) and the concentration of the fission and activation products in the fuel matrix. Computer models, such as the RMCC thermodynamic fuel model [2], can be used to predict the phase stability for a given condition as a function of temperature ( $T$ ),  $pO_2$ , and chemical inventory.

### 2.2 Oxidation of Activation and Fission Products

As the  $UO_2$  fuel fissions,  $O_2$  is freed and can oxidize the activation and fission products or remain in the uranium fuel matrix. Thermodynamics can be used to determine the species that will be oxidized or remain in the metallic phase. Recall that a reaction with a Gibbs energy change ( $\Delta G$ ) equal to zero is at equilibrium. When  $\Delta G < 0$ , the reaction is thermodynamically favoured in the forward direction. When  $\Delta G > 0$ , the reaction is thermodynamically favoured in the reverse direction [5]. A reaction where  $\Delta G \ll 0$  will be thermodynamically favoured over a reaction where  $\Delta G < 0$ , if both reactions require a mutual reactant. In the case of oxidation of activation and fission products, the activation and fission products compete with  $UO_2$  for the  $O_2$ . In the case of defective fuel, there is sufficiently more  $O_2$  present than in a non-defective element.

The competition for  $O_2$  is illustrated in the Ellingham diagram in Figure 1, which shows the isolated oxidation reactions of various species within the fuel matrix with one mole of  $O_2$ . An Ellingham diagram plots the change in  $\Delta G$  for the formation of the oxide as a function of  $T$ . The water formation line has also been included in Figure 1 because of the importance of water to the presence of  $O_2$  in defective fuel. In general, reactions below the  $H_2O$  formation line, such as the formation of  $ZrO_2$ , tend to proceed in the forward direction to form oxides in the presence of water as their oxidation is more thermodynamically favoured than that of  $H_2$ . Whereas reactions far above the  $H_2O$  line, such as the formation of  $PdO$ , tend to proceed in the reverse direction and remain in the metallic form.

---

\*Defective fuel rate is less than 0.1% per fuel bundle

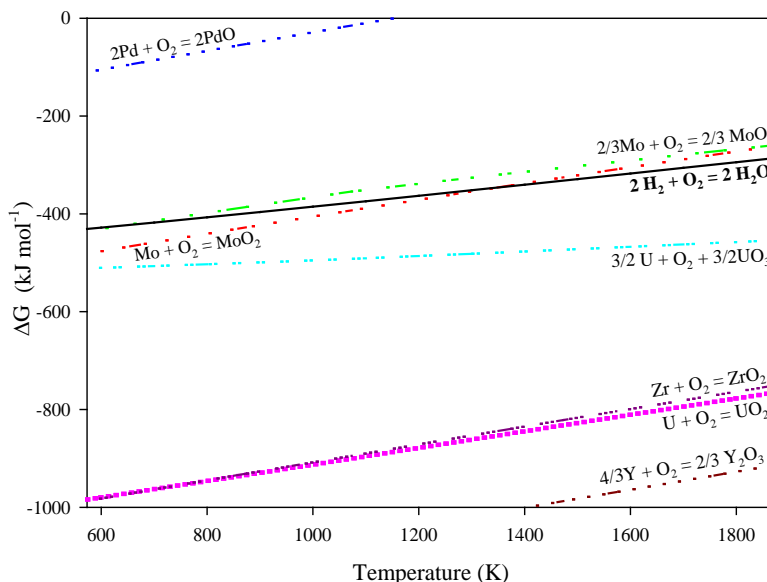


Figure 1: Ellingham diagram for the formation of select fuel related oxides with 1 mol  $O_2$  in relation to  $H_2O$  [6].

### 2.3 Molybdenum

While there are many fission and activation products that can be studied, this project focuses on the formation of  $Mo$ -oxides because of the ability of  $Mo$  to buffer  $O_2$  and exist as either a metal or an oxide depending on  $T$  and  $pO_2$ . This duality is best illustrated by the intersection of the  $MoO_2$  and  $H_2O$  formation lines in Figure 1, which is emphasized in Figure 2. It is possible that a relationship between the  $pO_2$  at a specific  $T$  and the metal to oxide ratio of  $Mo$  can be established.

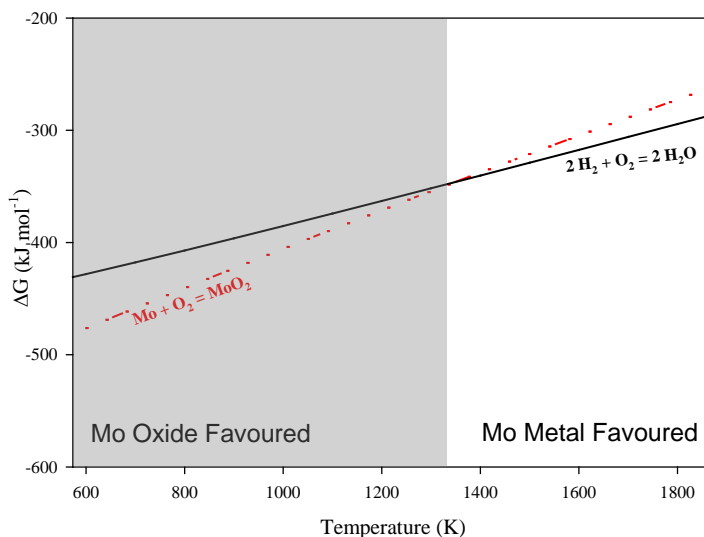


Figure 2: Ellingham diagram comparing the formation of  $H_2O$  and  $MoO_2$  [7]

### 2.3.1 Temperature Dependence

Temperature has an effect on the ability of *Mo* to buffer oxygen. First, consider the formation of *MoO*<sub>2</sub> at 800 K in Figure 2:

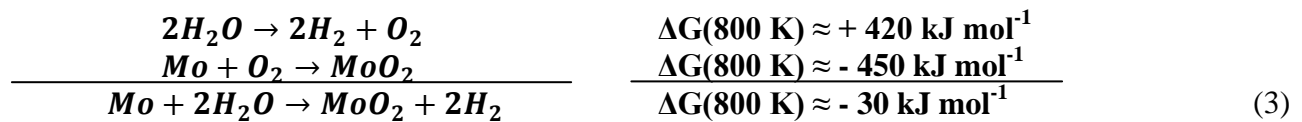


This reaction is favoured in isolation because it has a negative  $\Delta G$ .

However, *H*<sub>2</sub> is competing for the *O*<sub>2</sub> in the fuel element as well,

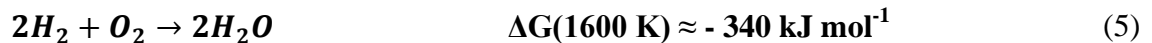
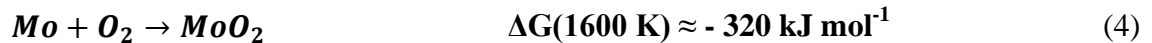


Reversing Equation (2) and adding it to Equation (1)

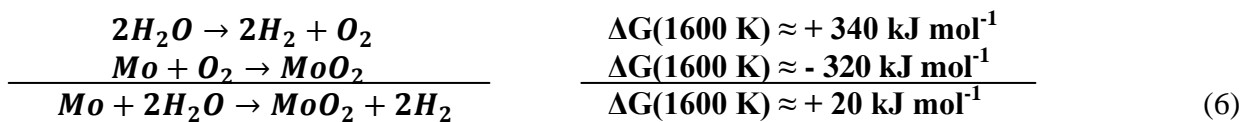


As seen in Equation (3), the oxidation of *Mo* by *H*<sub>2</sub>*O* is favoured at 800 K as the  $\Delta G$  is negative.

At 1600 K:



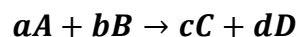
Therefore,



The oxidation of *Mo* over *H*<sub>2</sub> is not favoured at 1600 K. This reaction will occur in the opposite direction and metallic *Mo* will be favoured. Thus, temperature has an effect on the ability of molybdenum to buffer oxygen.

### 2.3.2 Oxygen Partial Pressure Dependence

The oxidation of *Mo* can be also represented as a function of oxygen partial pressure. Recall for a reaction of the form



The following thermodynamic relationship applies [5]

$$\Delta G = \Delta G^o + RT \ln \left( \frac{[C]^c [D]^d}{[A]^a [B]^b} \right) \quad (7)$$

Where  $T$  is the temperature in K and  $R$  is the universal gas constant. For the reaction of



Equation 7 is of the form

$$\Delta G_8 = \Delta G_8^o + RT \ln \left( \frac{a(MoO_2) p_{H_2}^2}{a(Mo) p_{H_2O}^2} \right) \quad (9)$$

As  $Mo$  and  $MoO_2$  both have an activity ( $a$ ) of unity, Equation (9) can be simplified to

$$\Delta G_8 = \Delta G_8^o + RT \ln \left( \frac{p_{H_2}^2}{p_{H_2O}^2} \right) \quad (10)$$

Equation (10) shows that the change in Gibbs energy for Equation 8,  $\Delta G_8$ , is related to the ratios of the partial pressures ( $p$ ) of  $H_2:H_2O$ . Thus, the favourability of the oxidation of  $Mo$  in the presence of water is dependent on the ratio of  $H_2:H_2O$  and  $T$ .

Recall that the  $\left( \frac{p_{H_2}^2}{p_{H_2O}^2} \right)$  is related to the  $p_{O_2}$  by the formation reaction for  $H_2O$



$$\Delta G_{11} = \Delta G_{11}^o + RT \ln \left( \frac{(p_{H_2O})^2}{(p_{O_2})(p_{H_2})^2} \right) \quad (12)$$

As  $\Delta G_{11}^o$  is equal to  $2\Delta G_{f,H_2O}^o$  and at equilibrium  $\Delta G_{11}$  is zero, the above can be re-arranged to

$$p_{O_2} = \left( \frac{p_{H_2}}{p_{H_2O}} \right)^{-2} e^{\left( \frac{2\Delta G_{f,H_2O}^o}{RT} \right)} \quad (13)$$

In summary, Equations 8 to 13 illustrate that the oxidation of  $Mo$  to  $MoO_2$  (in this case) is a function of  $p_{O_2}$ , which can be related to the ratio of the partial pressures of  $H_2:H_2O$ . As discussed in Section 3, the above equations are significant as all are specifically related to the planned experimentation.

## 2.4 Non-Stoichiometric Molybdenum

In addition to the complete oxidation and reduction of  $Mo$  from the metallic form to the oxide form and vice versa, shown in Equation (8), there exists a region of non-stoichiometry in the  $MoO_2$  crystal

structure during oxidation and reduction. Figure 3 is a binary phase diagram of  $Mo-O$ .  $MoO_2$  exists only when  $x_o=2/3$  exactly,  $x_o$  being the percentage of O atoms in the  $Mo-O$  system. This is surrounded by an area of non-stoichiometry, as marked in blue on Figure 3. To the left of  $x_o=2/3$  exists an area of hypo-stoichiometry,  $MoO_{2-X}^\dagger$ , and to the right of  $x_o=2/3$  exists an area of hyper-stoichiometry,  $MoO_{2+X}$ . This non-stoichiometry adds to molybdenum's ability to buffer  $O_2$  in the system, the extent of which is not well understood. Thus, this project will attempt to experimentally measure the extent of  $MoO_2$  non-stoichiometry as a function of  $pO_2$ .

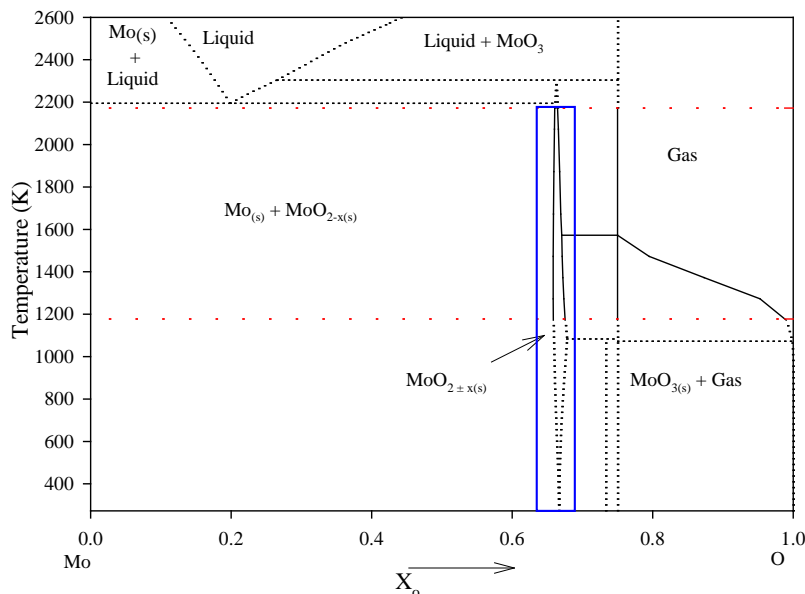


Figure 3:  $Mo-O$  binary phase diagram [6]

## 2.5 U-Mo-O Compounds

$Mo$  and  $O_2$  can combine with the  $UO_2$  fuel to create  $U-Mo-O$  compounds. These compounds can also play significant roles in oxygen buffering. This project puts an emphasis on  $UMoO_6$  as it has a formation line below the  $MoO_2$  formation line, as shown in Figure 4. This would suggest greater thermodynamic stability of this compound. As discussed in [2], it is believed that the formation of  $UMoO_6$  is important in correctly predicting fuel oxidation with the RMCC thermodynamic fuel model. This is because the  $UMoO_6$  compound stabilizes more moles of oxygen in the fuel matrix compared to the formation of  $MoO_2$  (e.g.,  $UMoO_6$ : three mol of  $O_2$  per mol of  $Mo$  compared to  $MoO_2$ : one mol of  $O_2$  per mol of  $Mo$ ). Reference [2] utilized literature values for the formation of  $MoO_2$ ,  $MoO_{2\pm X}$ , and  $UMoO_6$  in the fuel system. The purpose of this project is to gather experimental data to refine the thermodynamic database utilized by the RMCC thermodynamic fuel model. As discussed in the next section, experiments to determine the formation of  $MoO_2$ ,  $MoO_{2+X}$ , and  $UMoO_6$  as a function of  $pO_2$  and  $T$  will be completed.

<sup>†</sup>where  $X$  is the stoichiometric deviation of oxygen in  $MoO_2$ .

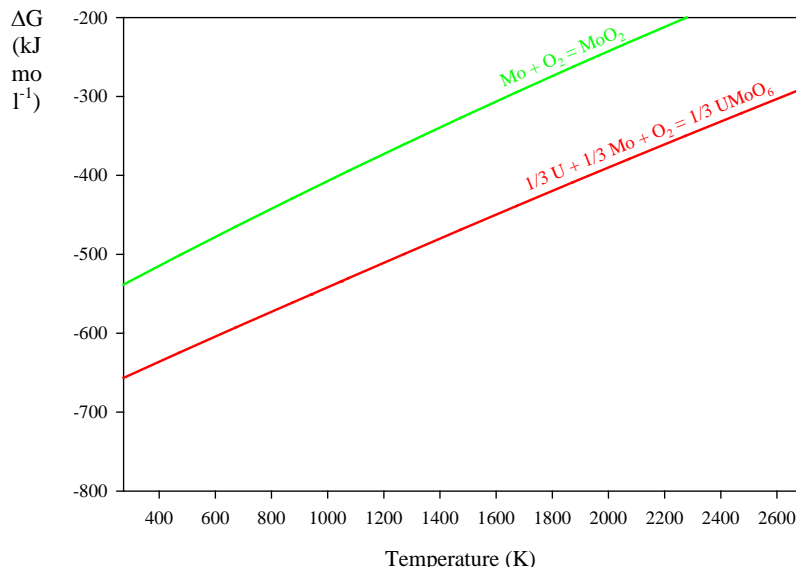


Figure 4: Ellingham diagram illustrating change in  $\Delta G$  for the formation of  $\text{MoO}_2$  and  $\text{UMoO}_6$  as a function of temperature [6]

### 3. Research Plan

The research will occur in three phases, (i) the  $\text{MoO}_{2+X}$  system, (ii) the  $\text{UMoO}_6$  system, and (iii) the integration of all results back into the RMCC thermodynamic fuel model.

#### 3.1 The $\text{MoO}_{2+X}$ System

A SETARAM SETSYS Evolution 24 Thermogravimetric Analysis / Differential Scanning Calorimetry (TGA/DSC) instrument will be used to gather mass change and heat flux data for samples of  $\text{MoO}_2$  held at a given  $T$  and  $p\text{O}_2$  over time. A sample of  $\text{MoO}_2$  will be placed in the TGA/DSC and reduced to pure  $\text{MoO}_2$  using an ultra-high purity  $\text{H}_2$  and argon ( $\text{Ar}$ ) carrier gas mixture, removing any  $\text{O}_2$  adhered to the surface. The sample will then be heated to 1273 K under a fixed  $p\text{O}_2$  cover gas. The sample will be allowed to equilibrate to  $\text{MoO}_{2+X}$ . Changes in mass and enthalpy will be measured as a function of time. The sample will be cooled and evaluated using X-ray Diffraction (XRD, (Thermo/ARL) Scintag X1) and Scanning Electron Microscopy (SEM, Philips XL-30CP). These tools will be used to confirm the presence of  $\text{MoO}_{2+X}$ . The sample will then be re-reduced to pure  $\text{MoO}_2$  to ensure no  $\text{Mo}$  is lost in the carrier gas as volatile species during the experiment.

The independent variable for this experiment is  $p\text{O}_2$ . The extremely small  $p\text{O}_2$ 's ( $10^{-19}$  to  $10^{-10}$  atm) required for these experiments will be generated using a Zirox SGM5 EL semi-conductor cell. The cell is used to introduce a known  $p\text{O}_2$  to the carrier gas mixture. The cell operates by introducing oxygen gas into the mixture, which converts some of the  $\text{H}_2$  to  $\text{H}_2\text{O}$ ; thus creating a small  $p\text{O}_2$  [6]. The  $\text{H}_2:\text{H}_2\text{O}$  ratio can be used to control the  $p\text{O}_2$  at a given temperature as shown by Equations 11 to 13. Figure 5 depicts the variation in  $p\text{O}_2$  over a wide range of temperature and  $\text{H}_2:\text{H}_2\text{O}$  ratios.

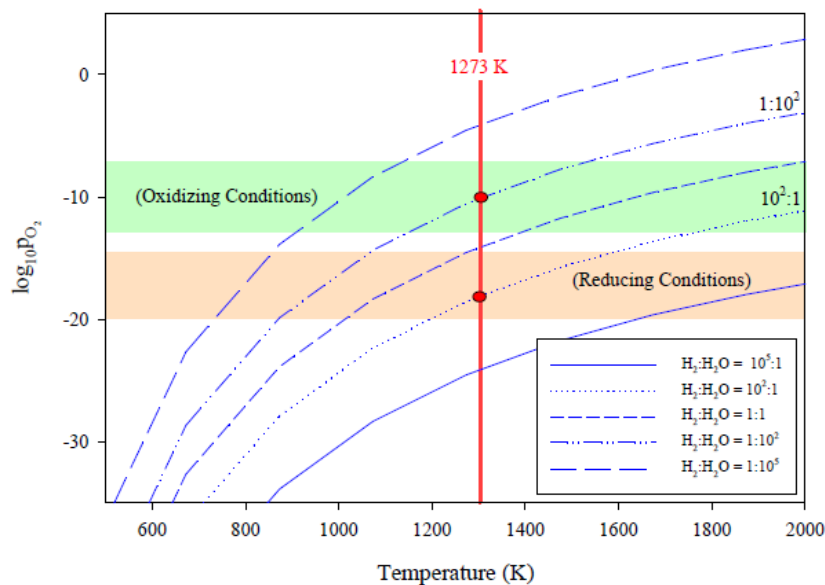


**Figure 5: Relationship between  $pO_2$  and  $H_2:H_2O$  over a range of temperatures [6]**

For these experiments, the independent variable of  $pO_2$  will be fixed using a  $H_2:H_2O$  ratio and the increase in mass will be measured by *TGA/DSC*. Assuming no mass loss of  $MoO_2$ , the mass change will correspond to the change in stoichiometry. Repetition of this experiment at various  $pO_2$ 's will establish a relationship between  $MoO_{2+x}$  and  $pO_2$ , which will assist in the modelling of the non-stoichiometry region in Figure 3. Finally, the *TGA/DSC* is capable of enthalpy change ( $\Delta H$ ) measurements, which can also be used to benchmark the RMCC thermodynamic fuel model.

Figure 6 is a visual schematic of the experimental setup showing the  $H_2$  and Ar carrier gas mixture, the Zirox cell inducing fixed  $H_2:H_2O$  (or known  $pO_2$ ), which oxidizes the  $MoO_2$  while the *TGA/DSC* measures enthalpy change and mass change.

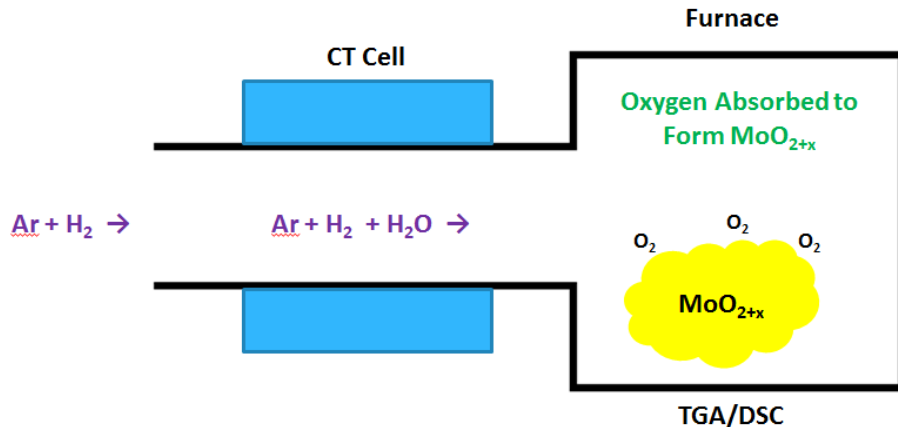


Figure 6: Schematic of experimental setup

Figure 7 depicts the range of oxidizing and reducing conditions that will be tested in this project ( $p\text{O}_2$ 's of  $10^{-19}$  to  $10^{-10}$  atm). Also depicted are the  $\text{H}_2:\text{H}_2\text{O}$  ratios required to create the  $p\text{O}_2$  conditions, defined by Equation (15). If all tests are run at 1273 K, shown by the vertical violet line, the metallic form will be favoured under “reducing conditions” and the oxide form will be favoured in “oxidizing conditions”.

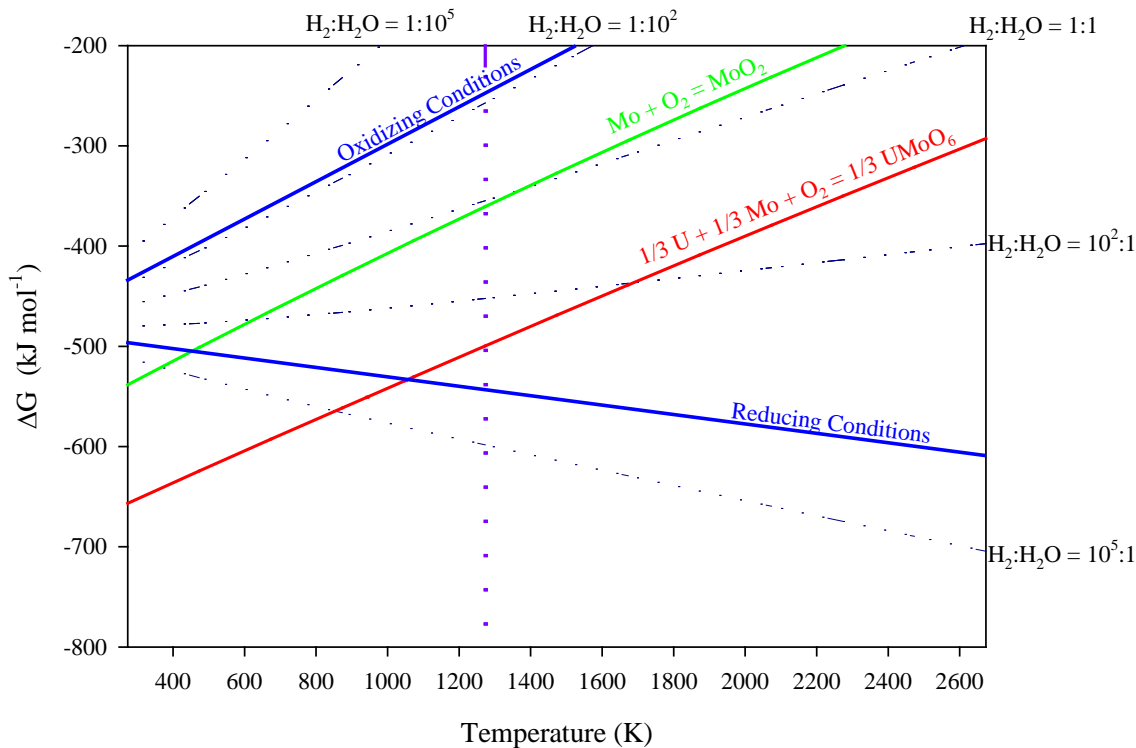


Figure 7: Ellingham diagram illustrating the range of  $p\text{O}_2$  to be tested and the change in  $\Delta G$  for the formation of  $\text{MoO}_2$  and  $\text{UMo}_6$ [6]

### 3.2 The $UMoO_6$ System

As mentioned in Section 2.5,  $UMoO_6$  is of interest as it is more stable than  $MoO_2$  (Figure 7) and stabilizes more moles of  $O_2$  per mole of  $Mo$  than  $MoO_2$ . Also,  $UMoO_6$  was incorporated into the RMCC thermodynamic fuel model because of its ability to rectify the model with experimental data [6]. The presence and formation of this compound under reactor conditions needs further experimental validation.

The experimental plan for the  $UMoO_6$  system is very similar to the  $MoO_{2+X}$  experimentation.  $UMoO_6$  will be synthesized in the lab using the method described by Bharadwaj *et al.* [8]. It will be placed in the TGA/DSC and, using a  $H_2$  and  $Ar$  carrier gas mixture, any  $O_2$  adhered to the surface will be driven off to ensure a pure  $UMoO_6$  sample. The sample will then be heated to 1273 K under a fixed  $pO_2$  cover gas. The sample will be allowed to equilibrate and its stability evaluated through changes in mass and enthalpy measured as a function of time. The sample will be cooled and evaluated using XRD and SEM. The sample will then be re-reduced to pure  $UMoO_6$  to ensure no  $Mo$  is lost in the carrier gas as volatile species during the experiment.

Further experiments will be attempted to create  $UMoO_6$  *in situ* by heating  $MoO_2$  and  $UO_2$  in the TGA/DSC and fixing a high  $pO_2$  cover gas. Mass change and enthalpy change over time will again be measured. The  $UMoO_6$  created *in situ* will be evaluated with XRD and SEM and compared to the synthesized  $UMoO_6$ .

### 3.3 The Integration of Results into the RMCC Thermodynamic Fuel Model

Experimental data on the effect of  $pO_2$  on  $MoO_{2+X}$  and  $UMoO_6$  will have been collected through enthalpy and mass measurements made by the TGA/DSC. Also, there will be some compositional data through XRD and SEM analysis. The mass and enthalpy data will be incorporated into the RMCC thermodynamic fuel model database. A clear relationship between  $pO_2$  and the metal to oxide ratio of  $Mo$  compounds ( $Mo : MoO_{2+X} : UMoO_6$ , *etc.*) will be established for potential use as a forensic tool to evaluate the propagation of oxygen through a defective fuel element on a microscopic level. Also, this relationship can potentially be used to confirm burnup by determining  $Mo$  concentration in the metal and oxide phases.

## 4. Summary

Using the above experimental plan, a relationship can be established between  $pO_2$  and the oxide to metal ratio of the  $U-Mo-O$  system (*i.e.*,  $Mo : MoO_{2+X} : UMoO_6$ , *etc.*). In future, this relationship could be used as a forensic tool to assist in mapping the propagation of  $O_2$  through defective fuels with higher spatial resolution or to confirm burnup. Also, this work will assist in advancing the RMCC thermodynamic fuel model, which supports the Canadian Nuclear Industry's effort of adequately predicting fuel behaviour.

## 5. Acknowledgements

The authors acknowledge the financial support of the Natural Science and Engineering Research Council of Canada, the CANDU Owners' Group, and the University Network of Excellence in Nuclear Engineering for financial support of this research effort. The authors are appreciative of the technical expertise and guidance of Atomic Energy of Canada Limited.

## References

- [1] J.D. Higgs, B.J. Lewis, W.T. Thompson and Z.He, “A Conceptual Model for the Fuel Oxidation of Defective Fuel”, *Journal of Nuclear Materials*, Vol. 366, 2007, pp.99-128.
- [2] E.C. Corcoran, B. J. Lewis, W. T. Thompson, J. Mouris and Z. He, “Controlled Oxidation Experiments of Simulated Irradiated UO<sub>2</sub> Fuel in Relation to Thermochemical Modelling”, *Journal of Nuclear Materials*, Vol. 414, Iss. 2, 2011, pp.73-82.
- [3] AECL “Status Report 69 – Advanced CANDU Reactor 1000 (ACR-1000)”, Status Report.<http://www.iaea.org/NuclearPower/Downloadable/aris/2013/4.ACR1000.pdf>
- [4] R.D. MacDonald, M.R. Floyd, B.J. Lewis, A.M. Manzer and P.T. Truant, “Detecting, Locating and Identifying Failed Fuel in Canadian Power Reactors,” AECL-9714, Atomic Energy of Canada Limited, February 1990.
- [5] D.R. Gaskell, “Introduction to the Thermodynamics of Materials – Fifth Edition”, Taylor and Francis Group, New York, 2008.
- [6] E.C. Corcoran, “Thermochemical Modelling of Advanced CANDU Reactor Fuel”, PhD Thesis, Royal Military College of Canada, March 2009.
- [7] E.C. Corcoran, B.J. Lewis, W.T. Thompson, J. Mouris, and Z. He, “Controlled Oxidation Experiments of Simulated Irradiated UO<sub>2</sub> Fuel in Relation to Thermochemical Modelling”, *Journal of Nuclear Materials*, Vol. 414, 2011, pp.73-82.
- [8] S.R. Bharadwaj, M. S. Chandrasekharaiah and S. R. Dharwadkar, “On the Solid State Synthesis of UMoO<sub>6</sub>”, *Journal of Materials Science Letters*, Vol. 3, 1984, pp.840-842.